This reaction is undoubtedly complicated by the reactivity of VO^{2+} toward both HSO_5^- and H_2O_2. We have found the former reaction to proceed quite rapidly, with a bimolecular rate constant of 13 M^{-1} s^{-1} at 24 °C in 1 M $HClO_4$. For initial VO^{2+} and HSO_5^- concentrations of 2.16×10^{-2} and 2.71×10^{-4} M, respectively, 5.09×10^{-4} M VO_2^+ is produced. We therefore conclude that any HSO_5^- formed from the fluoroxysulfate will rapidly and nearly quantitatively oxidize VO^{2+} to VO_2^+.

The reaction between VO^{2+} and H_2O_2 has been carefully studied by Brooks and Sicilio.[19] The reaction is complicated, but the rate is comparable to the reaction rates in Table IV. The reaction usually oxidizes less than 2 mol of VO^{2+}/mol of H_2O_2, and the stoichiometry varies considerably with experimental conditions. This variability may account for the variations in stoichiometry of the VO^{2+}–SO_4F^- reaction. Our isotopic results are consistent with the O_2 product deriving from oxidation of H_2O_2.

All in all, we do not have a very clear understanding of the VO^{2+}–SO_4F^- system. It does seem, however, that VO^{2+} is somewhat less reactive toward SO_4F^- than is Co^{2+}. It also differs from Co^{2+} in that it does not appear to scavenge the precursor of H_2O_2 formed in the decomposition of aqueous SO_4F^-. Since VO^{2+} is generally considered to be a much better reducing agent than Co^{2+}, these are rather remarkable conclusions.

General Observations

Perhaps the most surprising feature of the aqueous chemistry of fluoroxysulfate is the enormous selectivity that this oxidant displays in its reactions with reducing substrates. The fluoroxysulfate ion shows this selectivity despite its formidable thermodynamic oxidizing power.[3] The relative reactivities toward SO_4F^- of the reductants that have been studied to date stand in the order $ClO_2^- > Ag^+ >>> Co^{2+} > VO^{2+} > H_2O >>> Cr^{3+}$. It is clear that thermodynamic driving force is not a major factor in determining these reactivities, but at the present time we are not in a position to say what is.

The rapid oxidation of Ag^+ seems especially noteworthy, since it is thermodynamically the poorest reductant of all those studied. There appears to be very little in the way of an activation barrier to the oxidation of Ag^+. Even peroxydisulfate, which has barely enough thermodynamic oxidizing power to effect this oxidation, does so at a significant rate. We are not aware of any explanation that has been offered for this surprising redox lability of the Ag^+–Ag^{2+} couple.

From a practical standpoint, the use of Ag^+ as an oxidation catalyst considerably extends the range of oxidations that can be effected with the fluoroxysulfates and makes it seem likely that these salts will find significant application as chemical reagents.

At this time we can claim only the most rudimentary understanding of the uncatalyzed reactions between SO_4F^- and VO^{2+} or Co^{2+}. It appears that when the rate of reaction of fluoroxysulfate with a substrate is comparable to the rate of its reaction with water, the system can become extraordinarily complicated. This is undoubtedly due at least in part to the variety of products and intermediates that are formed in the course of the water reaction.

Acknowledgment. We wish to thank the Argonne Analytical Laboratory for its assistance. In particular, thanks are due to Mrs. A. G. Engelkemeir for the gas analyses by mass spectrometry, Mr. K. Jensen for the sulfate analyses, and Ms. Florence Williams for the fluoride analyses.

Registry No. SO_4F^-, 73347-64-5; Cr^{3+}, 16065-83-1; Co^{2+}, 22541-53-3; VO^{2+}, 20644-97-7; Ag^+, 14701-21-4.

(19) Brooks, H. B.; Sicilio, F. *Inorg. Chem.* **1971**, *10*, 2530.

Contribution from the Department of Chemistry, McMaster University, Hamilton, Ontario L8S 4M1, Canada

Preparation of the $XeOTeF_5^+$, $FXeFXeOTeF_5^+$, $XeF_2 \cdot BrOF_2^+$, and $XeOSO_2F^+$ Cations and Their Study by ^{129}Xe, ^{125}Te, and ^{19}F Pulse Fourier Transform NMR and Raman Spectroscopy[1]

NORMAN KELLER and GARY J. SCHROBILGEN*[2]

Received April 10, 1980

The reactions of $XeOTeF_5^+AsF_6^-$ with BrF_5 have been studied in solution by multinuclear NMR spectroscopy and shown to yield the new fluorine-bridged cations $FXeFXeOTeF_5^+$ and $XeF_2 \cdot BrOF_2^+$. The latter has also been isolated at low temperature as its AsF_6^- salt and characterized in the solid state by Raman spectroscopy. The previously reported $XeOTF_5^+$ cation has been more fully characterized by Raman spectroscopy of its AsF_6^- and $Sb_2F_{11}^-$ salts and by multinuclear NMR spectroscopy and its solution structure unambiguously established. ^{129}Xe and ^{19}F NMR evidence has also been obtained for the $XeOSO_2F^+$ cation by dissolving $XeOTeF_5^+AsF_6^-$ in HSO_3F.

Introduction

The pentafluoroorthotellurate group, $OTeF_5$, is capable of stabilizing the +2, +4, and +6 oxidation states of xenon[3-7] and is highly electronegative.[8] Sladky[3-5] has prepared and characterized several xenon(II) derivatives containing the $OTeF_5$ group according to the sequence of reactions given by eq 1–3. Both $FXeOTeF_5$ and $Xe(OTeF_5)_2$ have been char-

$$2HOTeF_5 + XeF_2 \rightarrow Xe(OTeF_5)_2 + 2HF \quad (1)$$

$$Xe(OTeF_5)_2 + XeF_2 \rightarrow 2FXeOTeF_5 \quad (2)$$

$$FXeOTeF_5 + AsF_5 \rightarrow XeOTeF_5^+AsF_6^- \quad (3)$$

acterized by ^{19}F[3,4] and ^{129}Xe[9] NMR and Raman[3,4] spectroscopy. Previous evidence for the $XeOTeF_5^+$ cation was based on the Raman spectrum of its AsF_6^- salt.[5] Prior to this present study of ours, no $OTeF_5$ and analogues of the V-shaped $Xe_2F_3^+$ cation had been reported. Sladky[4] has shown that $XeOTeF_5^+AsF_6^-$ and XeF_2 react at 60 °C according to eq 4.

(1) Presented at the IXth International Symposium on Fluorine Chemistry, Avignon, France, 1979.
(2) To whom correspondence should be addressed.
(3) Sladky, F. *Monatsh. Chem.* **1970**, *101*, 1559.
(4) Sladky, F. *Monatsh. Chem.* **1970**, *101*, 1571.
(5) Sladky, F. *Monatsh. Chem.* **1970**, *101*, 1578.
(6) Lentz, D.; Seppelt, K. *Angew. Chem., Int. Ed. Engl.* **1978**, *17*, 356.
(7) Lentz, D.; Seppelt, K. *Angew. Chem., Int. Ed. Engl.* **1979**, *18*, 66.
(8) Lentz, D.; Seppelt, K. *Angew. Chem., Int. Ed. Engl.* **1978**, *17*, 355.

(9) Seppelt, K.; Rupp, H. H. *Z. Anorg. Allg. Chem.* **1974**, *409*, 338.

0020-1669/81/1320-2118$01.25/0

$$XeOTeF_5^+AsF_6^- + 2XeF_2 \rightarrow Xe_2F_3^+AsF_6^- + FXeOTeF_5 \quad (4)$$

Neither $(F_5TeOXe)_2F^+$ nor $FXeOTeF_5^+$ was observed.

With the aim of extending the chemistry of the pentafluoroorthotellurates of xenon(II), we have undertaken studies concerned with (1) the $OTeF_5$ group's ability to participate in nonredox metathetical fluorinations and (2) displacement of the $OTeF_5$ group by a suitably strong protonic acid.

Results and Discussion

$XeOTeF_5^+AsF_6^-$ and $XeOTeF_5^+Sb_2F_{11}^-$. We have repeated Sladky's[5] synthesis of $XeOTeF_5^+AsF_6^-$, and, although the early Raman evidence strongly supports the salt formulation for this compound, no evidence exists for the discrete nature of the $XeOTeF_5^+$ cation in solution. Our Raman spectrum suggests the existence of a significant anion–cation interaction by means of a fluorine bridge in the solid compound. We have therefore undertaken the study of this interesting cation in solution by pulse Fourier transform NMR spectroscopy and have reexamined the vibrational spectrum of $XeOTeF_5^+AsF_6^-$ and that of the hitherto unreported $Sb_2F_{11}^-$ compound.

Dissolution of $XeOTeF_5^+AsF_6^-$ in SbF_5 at room temperature results in displacement of AsF_5 by the stronger fluoride acceptor SbF_5 and the formation of bright yellow-orange solutions of the $XeOTeF_5^+$ cation in SbF_5 solvent (eq 5).

$$XeOTeF_5^+AsF_6^- + nSbF_5 \rightarrow XeOTeF_5^+Sb_nF_{5n+1}^- + AsF_5 \quad (5)$$

(a) NMR Spectroscopy. The ^{19}F, ^{125}Te, and ^{129}Xe NMR parameters are reported for solutions of $XeOTeF_5^+$ in SbF_5 in Table I. The ^{19}F NMR spectrum (Figure 1a and structure I) consists of an AB_4 spectrum ($J_{F_a-F_b}/\nu_0\delta_{F_a-F_b} = 0.1497$) in the region of fluorine on tellurium(VI). Two sets of natural abundance ^{125}Te ($I = {}^1/_2$, 7.50%) satellites, arising from the spin–spin couplings $J_{^{125}Te-^{19}F_a}$ and $J_{^{125}Te-^{19}F_b}$ were also observed in the ^{19}F spectrum. The ^{125}Te NMR spectrum consisted of a single ^{125}Te environment comprised of an overlapping binomial doublet of quintets resulting from the spin–spin couplings $J_{^{125}Te-^{19}F_b}$ and $J_{^{125}Te-^{19}F_a}$ (Figure 1b). No spin–spin coupling between ^{125}Te and ^{129}Xe could be detected either in the ^{125}Te or in the ^{129}Xe NMR spectrum (discussed below). Close examination of the more intense transitions in the B_4 portion of the ^{19}F spectrum reveals satellite doublets possessing spacings of 18.5 Hz. The satellites are attributed to a long-range $^{129}Xe-^{19}F_b$ coupling and have been confirmed by recording the ^{129}Xe spectrum (Figure 1c). The ^{129}Xe spectrum consists of a single xenon environment in the xenon(II) region of the spectrum with a 1:4:6:4:1 quintet fine structure due to long-range spin–spin coupling between the four equivalent equatorial fluorines of the $OTeF_5$ group and ^{129}Xe. No $^{129}Xe-^{19}F_a$ coupling could be resolved in either the ^{129}Xe or the ^{19}F spectra.

Although a weak fluorine bridge is expected between the xenon atom and the $Sb_nF_{5n+1}^-$ anion in solution, the interaction, like that of XeF^+ in SbF_5 solution, is labile on the NMR time scale at room temperature and cannot be observed. The NMR findings are consistent with a discrete $XeOTeF_5^+$ cation possessing structure I in SbF_5 solution.

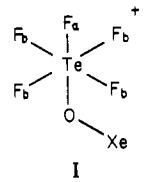

I

(b) Raman Spectroscopy. With the assumption of either C_s or C_1 symmetry for $XeOTeF_5^+$, a total of 18 Raman and infrared-active modes are predicted for the cation. Staggered or eclipsed conformations for the equatorial fluorines on tellurium and the xenon would yield 11 A′ + 7 A″ or 12 A′ + 6 A″, respectively, as the alternative vibrational representations under C_s symmetry. The two possible choices for the σ_h plane under C_s symmetry only affect ν_4, ν_{11}, and ν_{15} by interchanging irreducible representations to which they belong (Table II). Further reduction of the symmetry by assuming the gauche conformation under C_1 symmetry would yield 18 A as the vibrational representation. However, the staggered conformation (C_s symmetry) is assumed to be the most stable, and the Raman spectrum of $XeOTeF_5^+$ has been assigned accordingly.

The assignments for the Raman spectrum of the $XeOTeF_5^+$ cation (Figure 2a,b and Table II) are based mainly on the

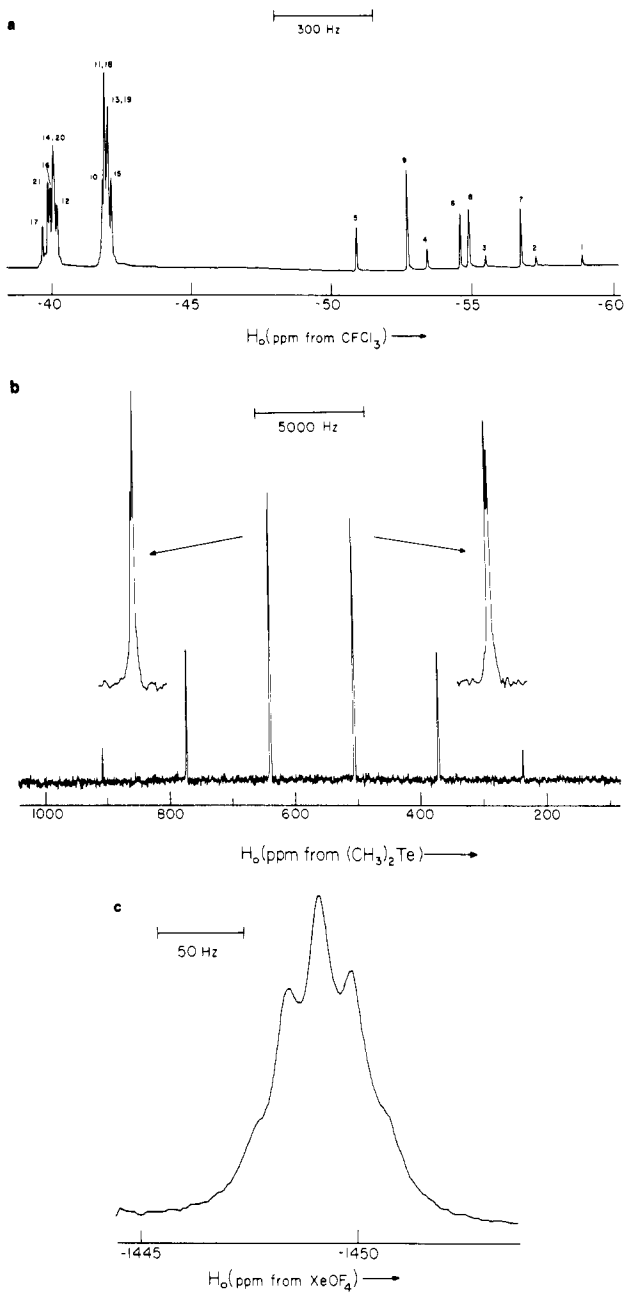

Figure 1. NMR spectra of $XeOTeF_5^+AsF_6^-$ recorded at 25 °C in SbF_5 solvent: (a) ^{19}F NMR spectrum (84.66 MHz, 0.295 *m*), where the numbering scheme for the observed transitions of the $OTeF_5$ group corresponds to that given for an AB_4 spin system in ref 33; (b) ^{125}Te NMR spectrum (28.43 MHz, 0.157 *m*), where only eight of the expected 10 lines of the multiplet are resolved; (c) ^{129}Xe NMR spectrum (24.90 MHz, 0.157 *m*), where only the equatorial fluorine on tellurium–xenon coupling is resolved.

Table I. NMR Parameters for $XeOTeF_5^+AsF_6^-$ in SbF_5, BrF_5, and HSO_3F Solvents

solvent	T, °C	species	chem shifts,[a] ppm				spin–spin coupling consts, Hz		
			$\delta_{^{19}F}$	$\delta_{^{129}Xe}$	$\delta_{^{125}Te}$	$\delta_{^{17}O}$	$J_{F-F'}$	$J_{^{129}Xe-^{19}F}$	$J_{^{125}Te-^{19}F}$
SbF_5[c]	25	$XeOTeF_4F'^+$	F, −41.0 F′, −54.6	−1472	−134.9		172.2 (AB_4)	F, 18.5[b] F′ [d]	F, 3814 (AB_4X) F′, 3802 (AB_4X)
		$SbF_5/Sb_nF_{5n+1}^-$	−111.2						
BrF_5[e,f]	−59	$FXeFBrOF_2^+$	F on Xe, −163.9 F on Br, 193.9	−1359				5680 (AX_2)	
		AsF_6^-	−58.1						
		TeF_6	−53.6		−165.9				3741 (AX_6)[g]
		BrF_5	F, 136.1 F′, 273.8				76.3 (AX_4)		
BrF_5[e,i]	−60	$FXeFXe'OTeF_4F'^+$	F on Xe[h] F on Xe′ [h]	Xe, −1146 Xe′, −1633				Xe, 5747 (AX_2) Xe′ [d]	
			F on Te F, −43.4 F′, −50.9				175.0 (AB_4)		F, 3697 (AB_4X) F′, 3767 (AB_4X)
		AsF_6^-	−60.2						
		TeF_6	−53.4						3741 (AX_6)[f]
		$BrOF_2^+/BrOF_3$	200.0						
		BrF_5	F, 136.2 F′, 273.6				[j]		
		$(FXe)_2F'^+$	[h]	−1059				F, 6662 (AMX) F′, 4828 (AMX)	
$HOSO_2F$[k]	−80	$XeOTeF_4F'^+$	F, −42.5 F′, −49.6	[k]			176.7 (AB_4)		F, 3766 (AB_4X) F′, 3658 (AB_4X)
		$HOTeF_4F'$	F, −49.2 F′, −44.4				180.2 (AB_4)		F, 3566 (AB_4X) F′, 3422 (AB_4X)
		AsF_6^-	−61.1						
		$HOSO_2F$	40.9						
$HOSO_2F$[l] + AsF_5	−78	$XeOTeF_4F'^+$	F, −42.9 F′, −51.5	[l]			171.0 (AB_4)		F, 3777 (AB_4X) F′, 3684 (AB_4X)
		AsF_6^-/AsF_5	−53.1						
		$HOSO_2F$	41.0						
neat	45	$HOTeF_4F'$	F, −47.0 F′, −44.5		−112.3	90.1	182.1 (AB_4)		F, 3577 (AB_4X) F′, 3491 (AB_4X)

[a] The chemical shift convention is that outlined by the IUPAC (*Pure Appl. Chem.* 1972, *29*, 627; 1976, *45*, 217); i.e., a positive chemical shift denotes a positive frequency and vice versa. All spectra were referenced externally: ^{19}F, neat $CFCl_3$ at the quoted temperature; ^{129}Xe, neat $XeOF_4$ at 25 °C; ^{125}Te, saturated aqueous $(HO)_6Te$ at 25 °C where the chemical shift conversion with respect to neat $(CH_3)_2Te$ is given by $\delta[(CH_3)_2Te] = \delta[(HO)_6Te] + 710.9$; ^{17}O, natural abundance H_2O at 25 °C. [b] Binomial quintet structure observed in the ^{129}Xe spectrum. [c] Arsenic pentafluoride was evolved according to eq 5 and removed under vacuum. Final molal concentrations of $XeOTeF_5^+$: 0.295 (^{19}F), 0.742 (^{129}Xe, ^{125}Te). [d] No coupling resolved. [e] Initial molal concentrations of $XeOTeF_5^+AsF_6^-$: ^{19}F, 0.50; ^{129}Xe, 0.305. [f] Solute dissolved at −48 °C and warmed to room temperature for 1 min prior to recording the spectra. [g] $J_{^{123}Te-^{19}F} = 3100$ Hz (AX_6). [h] Not observed due to intermediate fluorine exchange. [i] Solute dissolved at −48 °C, not warmed above −48 °C prior to recording the spectra. [j] Spin–spin coupling collapsed due to slow fluorine exchange. [k] Solute dissolved at −78 °C, not warmed above −65 °C prior to recording the spectra. Initial molal concentration of $XeOTeF_5^+AsF_6^-$ 0.521 (^{19}F). See Tables IV and V for ^{129}Xe spectra. [l] Solute dissolved at −78 °C, not warmed above −65 °C prior to recording the spectra. Molal concentration of $XeOTeF_5^+AsF_6^-$ 0.543; molal concentration of AsF_5 2.76 (^{19}F). See Table IV for ^{129}Xe spectrum.

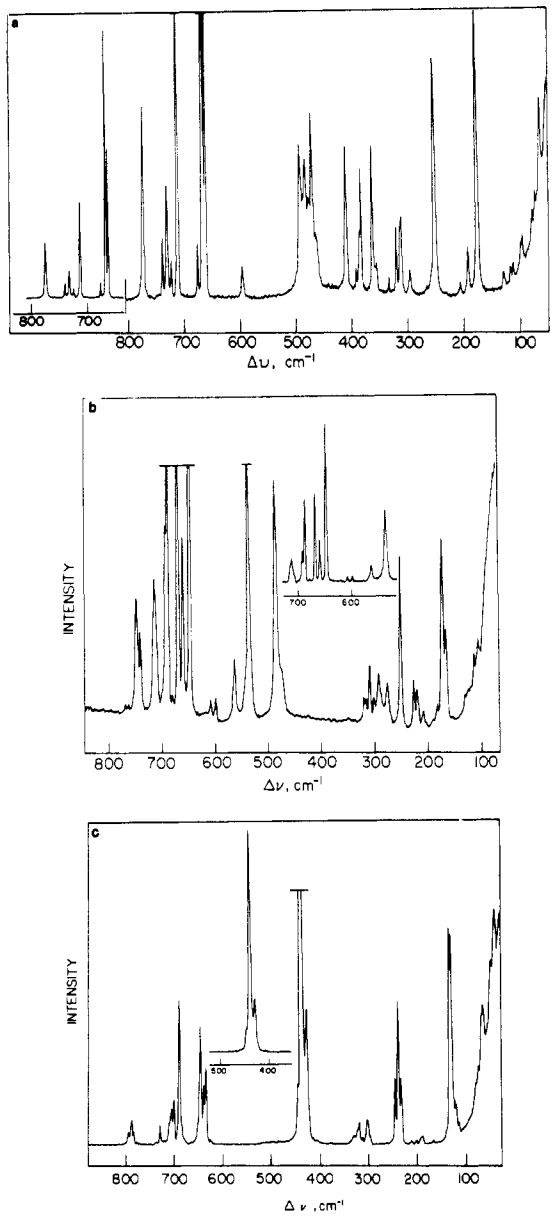

Figure 2. Raman spectra (−196 °C, 5145-Å excitation) of solid (a) $XeOTeF_5^+AsF_6^-$, (b) $XeOTeF_5^+Sb_2F_{11}^-$, and (c) $Xe(OTeF_5)_2$ recorded in glass.

assignments for the related C_{4v} molecule TeF_5Cl.[10] Although the vibrational spectrum of the $OTeF_5^-$ anion has been adequately assigned,[11] the net negative charge leads to a substantial drop in the Te–F stretching force constants and a large increase in the Te–O stretching force constant. It is assumed, however, that values of the stretching and bending force constants of the TeF_5 moieties in $XeOTeF_5^+$ and TeF_5Cl will not be significantly different. The assignments in Table II are consequently derived by correlating the relevant vibrational modes of TeF_5Cl under C_{4v} symmetry to those of $XeOTeF_5^+$ under C_s symmetry. The corresponding correlation of $OTeF_5^-$ is also presented for comparison.

The strongly coupled symmetric and asymmetric Te–O–Xe stretching frequencies of $XeOTeF_5^+$ are expected to occur at higher frequencies than in $FXeOTeF_5$ (457 cm^{-1})[4] and $Xe(OTeF_5)_2$ (440 and 428 cm^{-1}, this work) and are assigned to peaks occurring at 487 and 475 cm^{-1}, respectively. The present assignments for the Te–O–Xe stretches differ considerably from previous work. Although no explicit assignments for coupled Te–O–Xe stretches in $XeOTeF_5^+$ and $Xe(OTeF_5)_2$ had been made previously, bands attributed to discreet Te–O and Xe–O stretching modes had been assigned.[3-5] The Te–O stretch has been allotted to regions 200–300 cm^{-1} higher than we would anticipate. The assignment for the asymmetric Te–O stretch in $F_5TeOTeF_5$[12] (891 cm^{-1}) is also too high, but the assignment for the symmetric Te–O stretch (472 cm^{-1}) is in close agreement with our assignments of the Te–O–Xe stretches in $XeOTeF_5^+$. Like XeF^+, $XeOTeF_5^+$ possesses a xenon–ligand stretching frequency that is significantly higher than in the corresponding neutral bis-species. The frequency changes for the $Sb_2F_{11}^-$ compounds of $XeOTeF_5^+$ and XeF^+ are $\Delta\nu$(Xe–O) = 47 cm^{-1} and $\Delta\nu$(Xe–F) = 84 cm^{-1},[13] higher than in the respective parent molecules $Xe(OTeF_5)_2$ and XeF_2, and imply a significant increase in the xenon–ligand bond covalency with formal positive charge.

The Raman spectrum of the AsF_6^- anion in $XeOTeF_5^+AsF_6^-$ suggests that a significant Xe---F–As fluorine-bridge interaction exists. Thus, while three Raman-active modes are predicted for an AsF_6^- anion possessing O_h symmetry, 10 are actually observed which can be attributed to AsF_6^- and are presumed to arise from lowering of the anion symmetry from O_h to C_{4v} or a lower symmetry by means of a fluorine-bridge interaction. The vibrational modes of fluorine-bridged MF_6^- anions have been previously discussed and assigned on the basis of approximate C_{4v} symmetry for several XeF^+ and KrF^+ compounds.[14] However, site-symmetry lowering and vibrational coupling of the modes within the unit cell cannot be ruled out in the absence of crystal structure data. An analogous assignment is given in Table II for the anion modes of $XeOTeF_5^+AsF_6^-$. It is not clear, due to the complex nature of the $Sb_2F_{11}^-$ anion spectrum, whether or not the more weakly basic $Sb_2F_{11}^-$ anion of $XeOTeF_5^+Sb_2F_{11}^-$ is fluorine-bridged to the cation. No attempt has been made to assign the anion modes of $XeOTeF_5^+Sb_2F_{11}^-$.

$XeF_2 \cdot BrOF_2^+AsF_6^-$. The fluorination of $OTeF_5$ groups by the group 7 pentafluorides, (XF_5, where X = Cl, Br, or I) according to eq 6 would offer alternative syntheses for the

$$YOTeF_5^n + XF_5 \rightarrow YF_2 + XOF_{3-n} + TeF_6 \qquad (6)$$

pentavalent oxyhalides of group 7 (n = 0; Y = XeF or XeO-TeF_5) and their cations (n = +1; Y = Xe).

Although the oxyhalo species XOF_3 and XOF_2^+ have been prepared and characterized by more direct synthetic routes,[15-20] no information exists concerning the fluoride-acceptor strengths of XOF_3 and XOF_2^+ toward a covalent fluoride such as XeF_2, also generated in reaction 6. A number of adducts of XeF_2 with pentafluorides are known, i.e., $XeF_2 \cdot MF_5$, $XeF_2 \cdot MF_5$, and $2XeF_2 \cdot MF_5$, which have considerable ionic character and are thus written as $XeF^+MF_6^-$, $XeF^+M_2F_{11}^-$, and $Xe_2F_3^+MF_6^-$.[21] In the XeF^+ compounds there is a rather

(10) Brooks, W. V. F.; Eshaque, M.; Lau, C.; Passmore, J. *Can. J. Chem.* **1976**, *54*, 817.
(11) Mayer, E.; Sladky, F. *Inorg. Chem.* **1975**, *14*, 589.
(12) Bürger, J. *Z. Anorg. Allg. Chem.* **1968**, *360*, 97.
(13) Gillespie, R. J.; Landa, B. *Inorg. Chem.* **1973**, *12*, 1383.
(14) Gillespie, R. J.; Schrobilgen, G. J. *Inorg. Chem.* **1976**, *15*, 22.
(15) Christe, K. O.; Schack, C. J. *Adv. Inorg. Chem. Radiochem.* **1976**, *18*, 319.
(16) Gillespie, R. J.; Spekkens, P. H. *J. Chem. Soc., Dalton Trans.* **1977**, 1539.
(17) Bougon, R.; Bui Huy, T. *C. R. Hebd. Seances Acad. Sci., Ser. C* **1976**, *283*, 461.
(18) Bougon, R.; Bui Huy, T.; Charpin, P.; Gillespie, R. J.; Spekkens, P. H. *J. Chem. Soc., Dalton Trans.* **1979**, 6.
(19) Aynsley, E. E.; Nichols, R.; Robinson, P. L. *J. Chem. Soc.* **1953**, 623.
(20) Krasznai, J. P. Ph.D. Thesis, McMaster University, Hamilton, Ontario, Canada, 1975.

Table II. Raman Frequencies and Assignments for Some $XeOTeF_5^+$ Salts and $Xe(OTeF_5)_2$ Compared to Those of TeF_5Cl and $OTeF_5^-$

freq,[a] cm^{-1}							
$XeOTeF_5^+Sb_2F_{11}^-$	$XeOTeF_5^+AsF_6^-$	$Xe(OTeF_5)_2$[b]	assignt and approx description	freq, cm^{-1} TeF_5Cl[c]	assignt and approx description	freq, cm^{-1} $OTeF_5^-$[d]	assignt and approx description
748 (2)	739 (6)	730 (4)	a″, $\nu_{asym}(TeF_4)$, asym to plane of sym	726 (6)	ν_8(e), $\nu_{asym}(TeF_4)$	863 s	$\nu_1(a_1)$, ν(TeO)
741 (14)	775 (20)	796 (3), 788 (5), 785 (2)	a′, $\nu_{asym}(TeF_4)$, sym to plane of sym			637 vs	ν_8(e), $\nu_{asym}(TeF_4)$
714 (23)	713 (34)	710 sh, 708 sh, 706 (7), 701 (9)	a′, ν(TeF′)	708 (31)	$\nu_1(a_1)$, ν(TeF′)	581 m	$\nu_3(a_1)$, ν(TeF′)
671 (64)	668 (100)	690 (27)	a′, $\nu_{sym}(TeF_4)$, breathing	659 (100)	$\nu_2(a_1)$, $\nu_{sym}(TeF_4)$	650 vs	$\nu_2(a_1)$, $\nu_{sym}(TeF_4)$
661 (31)	663 (58)	647 (22), 639 (10), 635 (14)	a″, $\nu_{sym}(TeF_4)$, out of phase	651 (8)	$\nu_5(b_1)$, $\nu_{sym}(TeF_4)$, out of phase	664 sh	$\nu_5(b_1)$, $\nu_{sym}(TeF_4)$, out of phase
487 (41)	492 (16), 483 (14)	440 (100)[e], 445 sh	a′, ν_{sym}(XeOTe)				
474 sh	476 sh, 470 (18)	445 sh, 428 (27)[f]	a′, ν_{asym}(XeOTe)	410 (64)	$\nu_4(a_1)$, ν(TeCl)		
	333 (2)	332 (2), 328 (2)	a″, $\delta(F'TeF_4)$, out of plane of sym	327 (9)	ν_9(e), $\delta(F'TeF_4)$	347 w	ν_9(e), $\delta(F'TeF_4)$
320 (4)	320 (7)	320 (4)	a′, $\delta(F'TeF_4)$, in plane of sym				
311 (10)	312 (8)	304 (5)	a′, $\delta_{sym}(TeF_4)$, out of plane	312 (8)	$\nu_3(a_1)$, $\nu_{sym}(TeF_4)$, out of plane		
293 (9)	295 (3)	297 sh	a′, $\delta(TeF_4)$, in-plane scissors	302 (5)	$\nu_7(b_2)$, $\nu_{sym}(TeF_4)$, in plane	327 m	$\nu_7(b_2)$, $\delta_{sym}(TeF_4)$, in-plane
...	...	...	a′, $\delta_{asym}(TeF_4)$, sym to plane of sym				
252 (28)	252 (25)	247 (13), 240 (30), 234 (13)		259 (17)	ν_{10}(e), $\delta_{asym}(TeF_4)$, in plane		
...	...	...	a″, $\delta_{asym}(TeF_4)$, asym to plane of sym				
184 (4)	191 (5)	192 (2), 188 (2)	a′, $\delta(OTeF_4)$, in plane				
210 (3)	205 (1)	212 (1), 203 (1)	a″, $\delta(OTeF_4)$, out of plane	167 (18)	ν_{11}(e), $\delta(ClTeF_4)$	282 w	ν_{11}(e), $\delta(OTeF_4)$
...	...	...	a″, $\delta_{asym}(TeF_4)$, out of plane	199[h]	$\nu_6(b_1)$, $\delta_{asym}(TeF_4)$, out of plane		
173 (31)	174 (32)	136 sh, 133 (39), 130 (37)	a′, δ(XeOTe)				
...		...	a″, $\tau(Xe\text{-}O\text{-}TeF_5)$				
	365 (15)		ν(Xe---F)				
		123 (7), 120 (6), 115 (2), 66 (10),[g] 48 (9), 39 (11), 32 (11)					
694 (32)	731 (12)		ν_8(e), $\nu_{asym}(AsF_4)$				
691 (72)	724 (4)		$\nu_1(a_1)$, ν(AsF′)				
680 (4)	676 (6)		$\nu_2(a_1)$, $\nu_{sym}(AsF_4)$				
648 (100)	597 (3)		$\nu_4(a_1)$, ν(As---F)				
608 (3)	464 sh						
599 (4)	392 (2)		ν_{10}(e), $\delta_{asym}(AsF_4)$, in plane				
564 (11) } $Sb_2F_{11}^-$ (694–166)	386 sh		} ν_9(e), $\delta(F'AsF_4)$				
538 (48)	383 (12)						
316 (4)	356 (2)		$\nu_7(b_2)$, $\delta_{sym}(AsF_4)$, in plane				
302 (4)							
277 (7)	128 (12)						
227 (8)	116 (1)						
220 (6)	111 (1)						
166 (15)	98 (3) } g (128–63)						
132 (4)	96 (3)						
125 (4)	77 (2)						
114 (7) } g (132–77)	71 (2)						
106 (6)	63 (8)						
92 (8)							
77 (8)							

[a] Raman spectra of the solids were recorded at −196 °C in glass sample tubes with use of the 5145-Å exciting line. The resolution was 1.3 cm^{-1}. [b] The spectrum is assigned on the basis of C_s symmetry with assumption of small couplings between the $OTeF_5$ modes. However, additional small line splittings presumably arise from weak vibrational coupling between the $OTeF_5$ groups and/or coupling within the unit cell. A factor-group analysis using the crystal data of Sladky ($Z = 4$, space group D_{2h}^{8})[3] indicates that each Raman-active line will be split into a maximum of two components so that up to four splittings could be observed on each line. [c] Reference 10. [d] Reference 11. [e] ν_{sym}(XeOTe) in phase (440 cm^{-1}) and ν_{sym} (XeOTe) out of phase (445 cm^{-1}). [f] ν_{asym}(XeOTe) in phase (428 cm^{-1}) and ν_{asym}(XeOTe) out of phase (445 cm^{-1}). [g] External modes and/or low-frequency bending and torsional modes. [h] Calculated frequency.

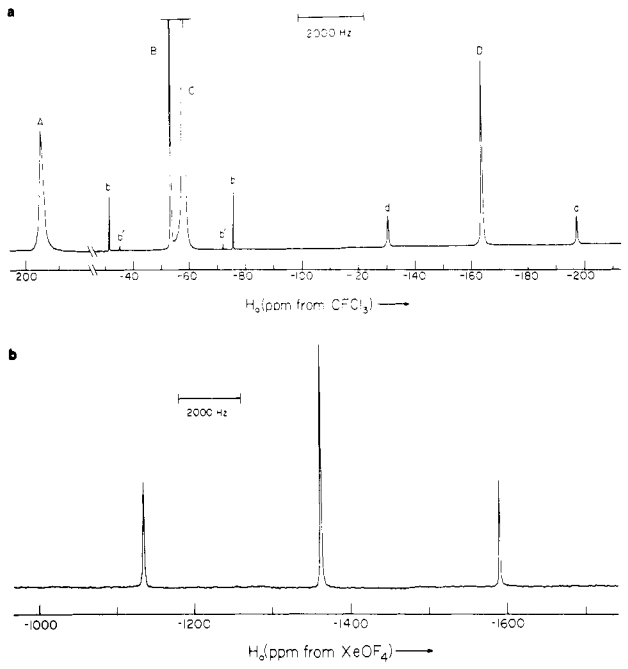

Figure 3. NMR spectra (−59 °C) of $XeOTeF_5^+AsF_6^-$ prepared at −48 °C in BrF_5 solvent and warmed to 25 °C for 1 min. (a) ^{19}F NMR spectrum (0.50 *m*) (solvent lines not shown): A, fluorine on bromine environment of the $FXeFBrO_2F^+$ cation; B, TeF_6 and ^{125}Te (b) and ^{123}Te (b′) satellites; C, AsF_6^-; D, fluorine-on-xenon environment of the $FXeFBrOF_2^+$ cation and ^{129}Xe satellites (d). (b) ^{129}Xe NMR spectrum (0.305 *m*).

strong covalent interaction between the anion and the cation giving rise to a fluorine bridge.[21,22]

More recently the adducts $XeF_2 \cdot MOF_4$ and $XeF_2 \cdot MOF_4$ have been prepared where M = Mo or W.[23,24] In the latter cases, the xenon–fluorine bridge bond lengths are considerably shorter than in the MF_5 adducts, approaching the Xe–F bond distance in free XeF_2. Fluorine-19 NMR studies reveal that, unlike the MF_5 adducts of XeF_2, the Xe–F---M bridges in the WOF_4 and $MoOF_4$ adducts are nonlabile on the NMR time scale in solution at low temperatures.[24] The group 7 oxyhalides would also be expected to fall into the category of weak acceptor species. In the present study, the metathetical fluorination of the $OTeF_5$ group of $XeOTeF_5^+$ provides a convenient synthetic route to the preparation and study of one member of this new class of weakly fluorine-bridged fluorohalate adducts of xenon difluoride by permitting the simultaneous generation of stoichiometric amounts of XOF_2^+ and XeF_2 (eq 6) in solution at low temperature.

(a) NMR Spectroscopy. Dissolution of $XeOTeF_5^+AsF_6^-$ in BrF_5 at −48 °C yields a bright yellow solution which, upon warming to room temperature for several seconds, reacts to give a colorless solution. Such solutions were found to be stable for up to several hours at room temperature in glass. The results of our low-temperature NMR studies of the colorless solutions are summarized in Table I. A ^{19}F NMR study reveals the presence of well-defined multiplet fine structure on both fluorine environments of the solvent, BrF_5, ruling out fluorine exchange involving the solvent. A single line at 193.9 ppm is consistent with fluorine on bromine(V),[18] while an intense line at −53.6 ppm can be unambiguously assigned to TeF_6 and displays both ^{123}Te and ^{125}Te satellites. The presence of TeF_6 is confirmed by the ^{125}Te NMR spectrum which shows a 1:6:15:20:15:6:1 septet with a coupling of 3740 Hz. A broad line at −58.1 ppm in the ^{19}F spectrum is assigned to the quadrupole-collapsed lines of the AsF_6^- anion. The presence of fluorine on xenon(II) is confirmed by the observation of a single high-field peak at −163.9 ppm with ^{129}Xe satellites.[26] The ^{129}Xe–^{19}F coupling (5682 Hz) is very similar to that recorded for XeF_2 in BrF_5 at the same temperature (5650 Hz), but the chemical shift is ca. 20 ppm to low field of that of XeF_2 in BrF_5 at the same temperature.[14] Integration of the ^{19}F spectrum yields the relative peak areas of fluorine on bromine(V):TeF_6:AsF_6^-:fluorine on xenon(II) = 1:3:3:1.

A 1:2:1 triplet is observed at −1358 ppm in the ^{129}Xe NMR spectrum (Figure 3b) with $J_{^{129}Xe-^{19}F} = 5680$ Hz, thus showing that two fluorines, which are chemically equivalent on the NMR time scale, are directly bonded to the xenon. Although XeF_2 possesses a ^{129}Xe–^{19}F coupling constant which is similar, the ^{129}Xe chemical shift of XeF_2 in BrF_5[25] at the same temperature occurs ca. 350 ppm to high field of the new xenon(II) environment. We must therefore conclude that the species responsible for the new ^{129}Xe and ^{19}F resonances is not free XeF_2. The low-field positions of both the ^{19}F on xenon(II) and the ^{129}Xe chemical shifts of the new species relative to XeF_2 suggests that, on the NMR time scale, both fluorines are involved in equivalent fluorine bridging.

We propose that the NMR spectral results are consistent with reaction 7 and the formation of the fluorine-bridged

$$XeOTeF_5^+AsF_6^- + BrF_5 \rightarrow TeF_6 + XeF_2 \cdot BrOF_2^+AsF_6^- \quad (7)$$

$XeF_2 \cdot BrOF_2^+$ cation. The low-field fluorine on bromine(V) resonance at 193.9 ppm can be readily assigned to the $BrOF_2$ group and is in close agreement with the corresponding peak in $BrOF_2^+$ which occurs at 192 ppm in HF solution.[18] The high-field fluorine on xenon(II) resonance and corresponding ^{129}Xe resonance may be assigned to the fluorine-bridged XeF_2 group in which the two fluorine on Xe(II) environments are exchange averaged. It is worth noting that the ^{129}Xe resonance is similar to those of the weakly fluorine-bridged species $FXeFWOF_4$ and $FXeFMoOF_4$ which occur at −1331 (−66 °C) and −1383 ppm (−80 °C), respectively, in BrF_5 solution.[24,25] The exchange behavior of $XeF_2 \cdot BrOF_2^+$ contrasts, however, with that of $FXeFMOF_4$ (M = Mo or W) in BrF_5 at similar temperatures. Fluorine-19 and xenon-129 NMR spectra of the XeF_2 groups of these species show two well-resolved ^{19}F environments, a fluorine–fluorine spin–spin coupling between the terminal and bridging fluorines, spin–spin coupling between the fluorines on the metal and the bridging fluorines, and two distinct directly bonded ^{129}Xe–^{19}F spin–spin couplings.[24,25]

The precise nature of the solution exchange process for $XeF_2 \cdot BrOF_2^+$ is not clear, although only two reasonable mechanisms can, individually or combined, render the bridging and terminal environments of a fluorine-bridged XeF_2 molecule equivalent and also preserve the ^{129}Xe–^{19}F spin–spin coupling interaction. The first alternative represents an intramolecular exchange. It seems likely that the XeF_2 molecule could be bonded either end-on or edge-on to give five- or six-coordination about the bromine and that these bonding alternatives give rise to fluxional behavior in solution (eq 8). The second possibility involves dissociation of the adduct followed by intermolecular exchange of XeF_2 (eq 9). Both the intramo-

(21) Bartlett, N.; Sladky, F. O. In "Comprehensive Inorganic Chemistry"; Trotman-Dickenson, A. F., Ed.; Pergamon Press: Oxford, 1973; Vol. 1, p 213.
(22) Reference 13 and references therein.
(23) (a) Holloway, J. H.; Schrobilgen, G. J.; Taylor, P. *J. Chem. Soc., Chem. Commun.* **1975**, 40. (b) Tucker, P. A.; Taylor, P. A.; Holloway, J. H.; Russell, D. R. *Acta Crystallogr., Sect. B* **1975**, *B31*, 906. (c) Schrobilgen, G. J.; Holloway, J. H. *Inorg. Chem.* **1981**, in press.
(24) Holloway, J. H.; Schrobilgen, G. J. *Inorg. Chem.* **1980**, *19*, 2632.
(25) Schrobilgen, G. J.; Holloway, J. H.; Granger, P.; Brevard, C. *Inorg. Chem.* **1978**, *17*, 980.
(26) Gillespie, R. J.; Netzer, A.; Schrobilgen, G. J. *Inorg. Chem.* **1974**, *13*, 1455.

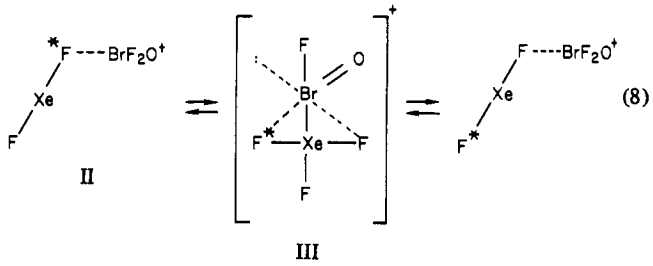

(8)

$$XeF_2 \cdot BrOF_2^+ \rightleftarrows XeF_2 + BrOF_2^+$$

$$*XeF_2 + XeF_2 \cdot BrOF_2^+ \rightleftarrows XeF_2 + (XeF_2)^* \cdot BrOF_2^+ \quad (9)$$

lecular and intermolecular exchange mechanisms also account for the absence of fluorine–fluorine spin–spin coupling between the fluorines on bromine and those on xenon.

From the solution behavior of the complex cation $XeF_2 \cdot BrOF_2^+$, it is clear that the XeF_2 molecule and $BrOF_2^+$ cation are associated through weak covalent fluorine bridging. The solid-state Raman spectra also support this conclusion.

(b) Raman Spectroscopy. Solid $XeF_2 \cdot BrOF_2^+AsF_6^-$ has been isolated from BrF_5 solutions of $XeOTeF_5^+AsF_6^-$ that had been previously warmed to room temperature for 1 min followed by removal of the solvent under vacuum at −48 °C. The solid compound is white to very pale yellow, melting at 0–5 °C and is very soluble in BrF_5 at −60 °C. This is in marked contrast to $BrOF_2^+AsF_6^-$, which exhibits only slight solubility in BrF_5 from room temperature to −60 °C. No analogous reaction was found to occur between IF_5 and $XeOTeF_5^+AsF_6^-$ at temperatures up to 70 °C.

The Raman spectrum of the solid has been recorded at −196 °C and is given in Figure 4. In the absence of an X-ray crystal structure, it has not been possible to conclusively demonstrate whether the XeF_2 group is bonded end-on (structure II) or edge-on (structure III) to Br in the $XeF_2 \cdot BrOF_2^+$ cation. Spectral assignments have been made on the basis of the end-on alternative and C_1 symmetry for the $FXeFBrOF_2^+$ cation in the present discussion. A total of 15 A-type Raman and infrared-active modes are expected for the cation. The assignments and the approximate descriptions of the vibrational modes are listed in Table III along with those for $BrOF_2^+AsF_6^-$.

It is clear from the vibrational spectrum that the geometry of the $BrOF_2$ group is similar to that of $BrOF_2^+$, and its modes are therefore readily assigned on the basis of the $BrOF_2^+AsF_6^-$ salt.[18] The occurrence of a Br=O stretch (1051 and 1045 cm^{-1}, factor-group split) at lower frequency than the corresponding stretch in $BrOF_2^+$ (1059 cm^{-1}) but at higher frequency than in $BrOF_3$ (1010 cm^{-1}) is consistent with fluorine bridging between $BrOF_2^+$ and XeF_2. The BrF_2 stretching modes, OBrF bends, and BrF_2 bends are similar to those of $BrOF_2^+$ and have been assigned accordingly.

The covalent nature of the fluorine-bridge bonds in $XeF_2 \cdot BrOF_2^+$ is substantiated by the observation of vibrational modes in the Raman spectrum which can be associated with the fluorine bridge(s). The bridged XeF_2 molecule may be regarded as distorted from $D_{\infty h}$ symmetry to C_s symmetry in $FXeFBrOF_2^+$. Consequently, the vibrational modes of free XeF_2 serve as a guide in rendering the assignment of the complexed XeF_2 molecule. The XeF_2 stretching modes under $D_{\infty h}$ symmetry occur at $\nu_1(\Sigma_g^+) = 497$ cm^{-1} and $\nu_3(\Sigma_u^+) = 555$ cm^{-1} and correlate to the bridging and terminal Xe–F stretching modes, respectively, under C_s symmetry while the doubly degenerate bending mode $\nu_2(\Pi_2) = 213$ cm^{-1} correlates with the in-plane and out-of-plane F–Xe---F bending modes of $FXeFBrOF_2^+$. The Raman spectrum of the linear F–Xe---F portion of the molecule is therefore characterized by a strong set of factor-group split lines at 546, 550, and 561 cm^{-1}

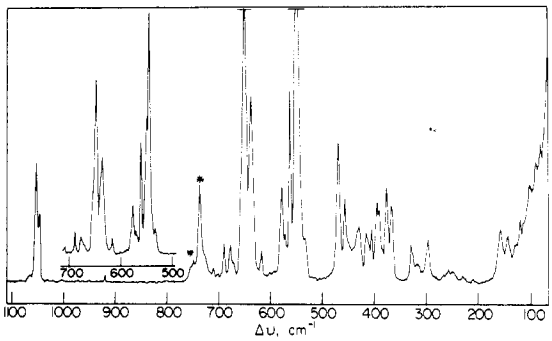

Figure 4. Raman spectrum (−196 °C, 5145-Å excitation) of solid $FXeFBrOF_2^+AsF_6^-$. Asterisks denote FEP sample tube lines.

assigned to the terminal Xe–F stretching mode. A weaker band at 468 cm^{-1} is assigned to the bridging Xe---F stretching mode. A pair of weak bands at 142 and 157 cm^{-1} are assigned to the two F–Xe---F bending modes expected for a molecule with a bent fluorine bridge. A comparison of the vibrational frequencies of the XeF_2 group of $FXeFBrOF_2^+$ with the equivalent frequencies of $(FXe)_2F^+$ and $FXeFMOF_4$ (M = Mo or W) supports our assignments and indicates that the fluorine-bridge interaction in $FXeFBrOF_2^+$ is weaker than in $FXeFMOF_4$: $(FXe)_2F^+$, 585, 418 and 162 cm^{-1};[13] $FXeFWOF_4$, 575, 458, and 153 cm^{-1};[23a,c] $FXeFMoOF_4$, 566, 450, and 152 cm^{-1}.[23a,c]

The presence of more than the three anticipated Raman-active modes for an octahedral AsF_6^- anion suggests that the anion is also involved in fluorine bridging to the $FXeFBrOF_2^+$ cation (structure IV). The anion spectrum has therefore been assigned, as in the previous discussion of $XeOTeF_5^+AsF_6^-$, on the basis of C_{4v} symmetry. The Raman results indicate that the AsF_6^- anion of $BrOF_2^+AsF_6^-$ is also distorted by a fluorine bridge interaction with the cation and has therefore been reassigned on the basis of C_{4v} symmetry[14] in Table III. Although the free $BrOF_2^+$ cation is expected to be trigonal pyramidal, the fluorine-bridged $BrOF_2^+$ cation in $BrOF_2^+AsF_6^-$ and $FXeFBrOF_2^+AsF_6^-$ should approximate to a trigonal-bipyramidal arrangement of four bonds and one lone pair and closely resemble the geometry of the $BrOF_2$ group depicted by structure IV.

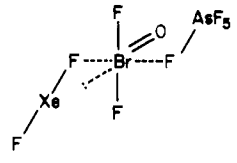

IV

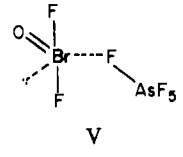

V

$FXeFXeOTeF_5^+$ Cation. We have noted earlier that dissolution of $XeOTeF_5^+AsF_6^-$ in BrF_5 at −48 °C yields a bright yellow solution which, when warmed, reacts to give colorless solutions of $XeF_2 \cdot BrOF_2^+AsF_6^-$. We have undertaken an investigation of the nature of the species responsible for the yellow color. Fluorine-19 NMR spectroscopy reveals that only partial fluorination of the available $OTeF_5$ groups has occurred at low temperature (Table I). An intense AB_4 pattern due to a single $OTeF_5$ environment is observed along with a very intense TeF_6 line. Both species display ^{125}Te satellite spectra. A broad line assigned to AsF_6^- and a sharp line assigned to fluorine on bromine(V) are also observed. The integrated relative intensities for fluorine on bromine(V), $OTeF_5$, TeF_6, and AsF_6^- were found to vary significantly from sample to sample. No fluorine on xenon(II) environments were, however, detected.

Owing to relatively slow xenon-exchange rates, the low-temperature ^{129}Xe spectra of unwarmed solutions of XeO-

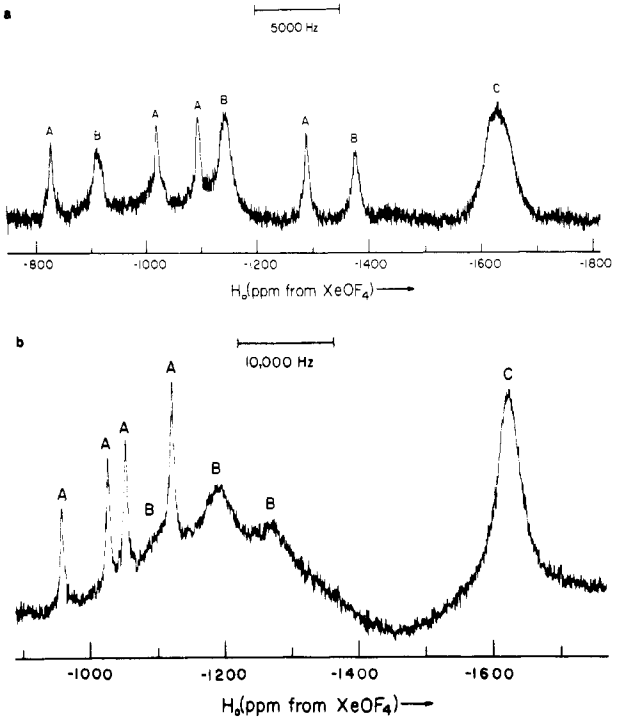

Figure 5. ^{129}Xe NMR spectrum of $XeOTeF_5^+AsF_6^-$ prepared in BrF_5 solvent at −48 °C and recorded at −60 °C: (a) 24.90 MHz, 0.305 *m*; (b) 62.90 MHz, 0.310 *m* (A, $Xe_2F_3^+$; B, XeF_2 group of $FXeFXeOTeF_5^+$; C, $XeOTeF_5$ group of $FXeFXeOTeF_5^+$).

$TeF_5^+AsF_6^-$ prepared in BrF_5 at −48 °C do, however, allow the observation of three $^{129}Xe(II)$ environments in these solutions (Table I and Figure 5). Their corresponding fluorine environments evidently cannot be detected in the ^{19}F spectra due to intermediate rates of fluorine exchange which severely broaden and collapse the environments into the spectral base line. The three $^{129}Xe(II)$ environments consist of a well-resolved 1:2:1 triplet, a binomial doublet of doublets, and a broadened singlet. The doublet of doublets is readily assigned to the $Xe_2F_3^+$ cation whose low-temperature ^{129}Xe spectrum in BrF_5 has been reported previously.[25] The low-field triplet possesses a ^{129}Xe–^{19}F coupling (5747 Hz) indicative of spin–spin coupling to two fluorines that are equivalent on the NMR time scale. However, the triplet chemical shift (−1146 ppm) occurs ca. 225 ppm to low field of $XeF_2{\cdot}BrOF_2^+$ and 575 ppm to low field of free XeF_2 in BrF_5 at comparable temperatures and concentrations. The high-field singlet has an intensity equal to that of the triplet and is assigned to a xenon bonded to an $OTeF_5$ group. The $OTeF_5$ group observed in the ^{19}F spectrum and the two new ^{129}Xe environments are consistent with the formation of the new fluorine-bridged cation $FXeFXeOTeF_5^+$ (structure VI). The Xe–F bond in structure

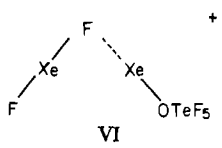

VI

VI is deemed to be labile by application of the same mechanisms discussed earlier for $XeF_2{\cdot}BrOF_2^+$. The reactions represented by eq 10 and 11 are consistent with the observed

$$2XeOTeF_5^+AsF_6^- + BrF_5 \rightarrow TeF_6 + FXeFXeOTeF_5^+AsF_6^- + BrOF_2^+AsF_6^- \quad (10)$$

$$FXeFXeOTeF_5^+AsF_6^- + BrF_5 \rightarrow TeF_6 + Xe_2F_3^+AsF_6^- + BrOF_3 \quad (11)$$

^{19}F and ^{129}Xe spectra. Separate environments are not observed for $BrOF_3$ and $BrOF_2^+$ in the ^{19}F spectrum owing to a rapid fluorine exchange between $BrOF_2^+$ and $BrOF_3$ involving equilibrium 12. Equilibrium 12 is presumably also indirectly

$$BrOF_2^+ + AsF_6^- \rightleftarrows BrOF_3 + AsF_5 \quad (12)$$

responsible for exchange broadening of the AsF_6^- and BrF_5 solvent lines according to equilibria 13 and 14.

$$BrF_5 + AsF_5 \rightleftarrows BrF_4^+ + AsF_6^- \quad (13)$$

$$*AsF_5 + AsF_6^- \rightleftarrows *AsF_6^- + AsF_5 \quad (14)$$

A considerable difference between the exchange behavior of $Xe_2F_3^+$ and $FXeFXeOTeF_5^+$ is noted and is underlined by the fact that both species have been observed in the same sample (Figure 5). The nonlabile behavior of Xe---F bonds of the symmetrically fluorine-bridged $Xe_2F_3^+$ cation is in contrast to that of $FXeFXeOTeF_5^+$ (structure VI). Valence-bond structure VIIa is apparently stabilized by the lower

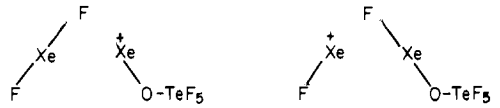

VIIa VIIb

effective electronegativity of the $OTeF_5$ group and is, in large measure, responsible for exchange averaging of the terminal and bridging fluorine on xenon environments of the $FXeFXeOTeF_5^+$ cation. Although it has not been possible to obtain the limiting spectra of either $XeF_2{\cdot}BrOF_2^+$ or $FXeFXeOTeF_5^+$, it has been possible to slow the exchange of XeF_2 in the ^{129}Xe spectrum of the latter cation by recording its spectrum at higher field strength. A comparison of the triplet line widths in Figure 5a (24.90 MHz) and Figure 5b (69.20 MHz) indicates that slowing of the exchange at higher field strength has occurred, supporting the structure proposed for the $FXeFXeOTeF_5^+$ cation.

Equations 10 and 11 may be viewed as the first two of three intermediate reactions leading to the formation of the $XeF_2{\cdot}BrOF_2^+$ cation from $XeOTeF_5^+$. The final reaction, represented by eq 15 is rapid at room temperature and yields,

$$Xe_2F_3^+AsF_6^- + BrOF_3 + BrOF_2^+AsF_6^- \rightarrow 2XeF_2{\cdot}BrOF_2^+AsF_6^- \quad (15)$$

upon removal of TeF_6 and BrF_5 solvent at −48 °C, pure $XeF_2{\cdot}BrOF_2^+AsF_6^-$.

$XeOSO_2F^+$ Cation. Previous attempts to prepare compounds of the $XeOSO_2F^+$ cation by reaction of XeF^+ compounds with HSO_3F in HF were not successful.[27] Our attempts to prepare the cation by the direct interaction of $FXeSO_3F$ with AsF_5 at −78 °C have led to the formation of a mixture of $S_2O_6F_2$, $(FXe)_2SO_3F^+AsF_6^-$, and $XeF^+AsF_6^-$.

Pentafluoroorthotelluric acid, $HOTeF_5$, possesses an acidity which is apparently less than that of HF and is thus readily displaced from its compounds by HF,[3,4] suggesting that F is more electronegative than $OTeF_5$. It is anticipated that HSO_3F, which possesses a Hammett acidity similar to that of HF (~15),[28] should also be capable of displacing $HOTeF_5$ from its compounds. We have, therefore, undertaken a study of the behavior of the $XeOTeF_5^+$ cation in HSO_3F solvent at low temperatures with the view in mind of obtaining evidence for the previously unreported and apparently very reactive $XeOSO_2F^+$ cation.

(27) Wechsberg, M.; Bulliner, P. A.; Sladky, F. O.; Mews, R.; Bartlett, N. *Inorg. Chem.* **1972**, *11*, 3063.
(28) Liang, J. Ph.D. Thesis, McMaster University, Hamilton, Ontario, Canada, 1976.

Table III. Raman Frequencies and Assignments for $FXeFBrOF_2^+AsF_6^-$ Compared to Those of $BrOF_2^+AsF_6^-$

$FXeBrOF_2^+AsF_6^-$ [a]		$BrOF_2^+AsF_6^-$ [b]		
freq, cm^{-1}	assignt	freq, cm^{-1}	assignt	approx description
1051 (29), 1045 (17)	$\nu_1(a)$	1059 (50)	$\nu_1(a')$	$\nu(Br{=}O)$
648 (72)	$\nu_2(a)$	649 (100)	$\nu_2(a')$	$\nu_{sym}(BrF_2)$
636 (40)	$\nu_{13}(a)$	634 sh	$\nu_5(a'')$	$\nu_{asym}(BrF_2)$
561 (46), 550 (57), 546 (100)	$\nu_3(a)$			$\nu(Xe{-}F)$
468 (32)	$\nu_4(a)$			$\nu(Xe{\cdots}F)$
404 (12)	$\nu_5(a)$			$\nu(Br{\cdots}F)$
375 (2)	$\nu_6(a)$	360 (18)	$\nu_3(a')$	$\delta_{sym}(OBrF)$
328 (8), 317 (4)	$\nu_{14}(a)$	311 (18)	$\nu_6(a'')$	$\delta_{asym}(OBrF)$
295 (10)	$\nu_7(a)$	289 (6)	$\nu_4(a')$	$\delta(BrF_2)$
229 (1)	$\nu_8(a)$			$\delta(OBr{\cdots}F)$
209 (1)	$\nu_9(a)$			$\delta(F{-}Br{\cdots}F)$
157 (10)	$\nu_{10}(a)$			$\delta_{sym}(FXe{\cdots}F)$
142 (6)	$\nu_{15}(a)$			$\delta_{asym}(FXe{\cdots}F)$
754 (3), 747 (5), 708 (3), 701 (1)		720 (17)	$\nu_8(e)$	$\nu_{asym}(AsF_4)$
688 (8), 676 (3), 670 (3)		688 (1)	$\nu_1(a_1)$	$\nu(AsF')$
576 (20), 571 (10)			$\nu_2(a_1)$	$\nu_{sym}(AsF_4)$
533 (9)		558 sh, 531 (12)	$\nu_5(b_1)$	$\nu_{sym}(AsF_4)$, out of phase
456 (19)			$\nu_4(a)$	$\nu(As{\cdots}F)$
428 (12)			$\nu_3(a_1)$	$\delta_{sym}(AsF_4)$, out of plane
414 (11)			$\nu_{10}(e)$	$\delta_{asym}(AsF_4)$, in plane
394 (18), 389 (16)		398 (1), 387 (6)	$\nu_9(e)$	$\delta(AsF_4)$
367 (17)			$\nu_7(b_2)$	$\delta_{sym}(AsF_4)$, in plane
257 (3), 248 (3)		239 (1)	$\nu_{11}(e)$	$\delta(F'AsF_4)$
127 (2)	$\nu_{11}(a)$, $\delta(Xe{\cdots}F{\cdots}Br)$	119 (4)	low frequency bends and torsional and lattice modes	
118 (4), 101 (6), 88 (5), 79 (6)	$\nu_{12}(a)$, $\tau(Xe{\cdots}F{\cdots}Br)$, $\delta(As{\cdots}F'{\cdots}Br)$, $\tau(As{\cdots}F'{\cdots}Br)$, and lattice modes	96 (10), 81, 44 (8)		

[a] The Raman spectrum of the solid was recorded at −196 °C in an FEP tube; sample tube lines have been deleted from the spectrum. The resolution was 1.3 cm^{-1}. [b] Reference 18.

Solutions of $XeOTeF_5^+AsF_6^-$ in HSO_3F are stable below −10 °C. A ^{19}F NMR study (Table I) shows that in addition to the solvent peak, unwarmed solutions of $XeOTeF_5^+AsF_6^-$ give rise to two AB_4 spectra of nearly equal intensities with ^{125}Te satellites at low temperature. These spectra are assigned to the TeF_5 groups of $HOTeF_5$ (confirmed by recording the spectrum of pure $HOTeF_5$ in HSO_3F solvent at −80 °C) and $XeOTeF_5^+$. No peaks other than the solvent peak and a broad peak due to fluorine on arsenic were observed. Tellurium-125 NMR spectra of these solutions fully corroborate the ^{19}F NMR results, as they show two overlapping doublets of quintets corresponding to $HOTeF_5$ and $XeOTeF_5^+$ (Table I).

The ^{125}Te and ^{19}F spectra are consistent with displacement of $HOTeF_5$ from the $XeOTeF_5^+$ cation by the stronger protonic acid HSO_3F to give the previously unreported $XeOSO_2F^+$ cation (eq 16 and structure VIII). Moreover, the

$$HOSO_2F + XeOTeF_5^+ \rightleftarrows HOTeF_5 + XeOSO_2F^+ \quad (16)$$

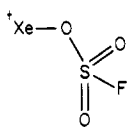

VIII

initial presence of $HOTeF_5$ rules out the possibility that the mixed species $FSO_2OXeOTeF_5$ is formed (equilibrium 17).

$$XeOTeF_5^+ + 2HOSO_2F \rightleftarrows FSO_2OXeOTeF_5 + H_2SO_3F^+ \quad (17)$$

No separate ^{19}F NMR peak was observed for the fluorine on sulfur of $XeOSO_2F^+$, which may either overlap with the HSO_3F solvent peak or may undergo rapid exchange averaging with the solvent according to equilibrium 18.

$$^+Xe(OSO_2F)^* + HOSO_2F \rightleftarrows XeOSO_2F^+ + H(OSO_2F)^* \quad (18)$$

Our assignments of the ^{19}F and ^{129}Xe spectra were confirmed by recording the spectra of HSO_3F solutions of $XeOTeF_5^+$ in the presence of excess Lewis acid. A 5:1 AsF_5:$XeOTeF_5^+$ mole ratio completely suppresses equilibrium 16 at −80 °C, showing only the $XeOTeF_5^+$ cation in the ^{19}F spectrum. Raising the temperature results in exchange broadening of the $OTeF_5$ peaks and the appearance of a broad set of peaks due to $HOTeF_5$. Line broadening due to slow chemical exchange in the ^{19}F spectrum is presumed to arise from equilibrium 19. The ^{129}Xe spectrum of $XeOTeF_5^+$ in

$$^+Xe(OTeF_5)^* + HOTeF_5 \rightleftarrows XeOTeF_5^+ + H(OTeF_5)^* \quad (19)$$

Table IV. Variable-Temperature ^{129}Xe NMR Study of $XeOTeF_5^+AsF_6^-$ in HSO_3F Solvent

	temp, °C	$\delta_{^{129}Xe}$	$w_{1/2}$, Hz	low-field peak intensity/ $XeOTeF_5^+$ peak intensity
0.378 *m* $XeOTeF_5^+AsF_6^-$, 1.94 *m* AsF_5	−80.8	−1564[a]	325	
	−65.5	−1571[a]	125	
	−50.0	−1578[a]	100	0.29
		−1303[b-d]	520	
	−33.8	−1586[a]	100	0.36
		−1313[b-d]	275	
	−20.9	−1591[a]	135	0.40
		−1320[b]	290	
	−10.6	−1596[a]	240	0.47
		−1328[b-d]	500	
0.266 *m* $XeOTeF_5^+AsF_6^-$	−94.6	−1521[a]	570	0.35
		−1426[b]	550	
	−80.0	−1536[a]	215	0.42
		−1453[b]	535	
	−73.8	−1541[a]	150	0.26
		−1450[b]	860	
	−66.4	−1546[a]	110	
	−49.8	−1559[a]	90	
	−33.0	−1573[a]	110	0.48
		−1389[b-d]	810	
	−20.2	−1584[a]	205	0.66
		−1411[b]	550	
	−10.0	−1596[a]	365	2.44
		−1428[b]	425	
1.07 *m* $XeOTeF_5^+AsF_6^-$	−31.7	−1586[a]	125	0.57
		−1286[c]	970	
	−20.2	−1595[a]	180	0.76
		−1278[c]	620	
	−9.2	−1605[a]	370	0.84
		−1287[c]	595	
	3.0	−1608[a]	620	1.06
		−1306[c]	950	

[a] $XeOTeF_5^+$. [b] $Xe(OSO_2F)_2$. [c] $XeOSO_2F^+$. [d] ^{129}Xe environments are exchange averaged.

the presence of a fivefold excess of AsF_5 displays only one peak due to $XeOTeF_5^+$ at −80 °C (Table IV). As the temperature is increased, another peak appears to low field and increases in intensity with increasing temperature. The new peak is assigned to the $XeOSO_2F^+$ cation and, like its analogues, XeF^+ and $XeOTeF_5^+$, possesses a ^{129}Xe chemical shift significantly to low field of those of its parent molecules, $FXeOSO_2F$ (−1416 ppm, −90 °C) and $Xe(OSO_2F)_2$ (−1572 ppm, −90 °C).[25] Xenon-129 chemical shifts of xenon(II) species are, in general, exceptionally sensitive to solvent and temperature effects. The observed decreases in chemical shifts of $XeOSO_2F^+$ and $XeOTeF_5^+$ with increasing temperature parallel previously reported behavior for a wide range of xenon(II) species.[25]

In the absence of AsF_5, the ^{129}Xe chemical shift behavior of the $XeOSO_2F^+$ cation is found to be more complex (Table IV). The ^{129}Xe NMR results support the ^{19}F NMR findings and indicate that equilibrium 16 is not completely suppressed even at −80 °C. In addition, the chemical shift of the low-field peak consistently occurs at considerably higher fields than in solutions acidified with AsF_5 (Table IV). This resonance displays the usual decrease in chemical shift with increasing temperature but broadens to such an extent at higher temperatures (−66 to −50 °C) that the signal is no longer visible. Further increases in the temperature result in the reappearance of a sharper peak at a lower field than was initially observed. The chemical shift again decreases while its intensity relative to $XeOTeF_5^+$ increases with increasing temperature. The $XeOTeF_5^+$ resonance, on the other hand, shows the normal temperature dependence, shifting to higher field with increasing temperature. This behavior is consistent with solvolysis of $XeOSO_2F^+$ according to equilibrium 20 to give

$$XeOSO_2F^+ + 2HSO_3F \rightleftarrows Xe(OSO_2F)_2 + H_2SO_3F^+ \quad (20)$$

$Xe(OSO_2F)_2$ and ensuing rapid xenon exchange between both species. It is reasonable to assume that equilibrium 20 also contributes to the lability of the SO_3F group of $XeOSO_2F^+$ in the ^{19}F NMR spectrum. At the lowest temperatures investigated for dilute solutions not containing AsF_5 (Table IV), equilibrium 20 apparently lies to the right. The chemical shift of the low-field species in these solutions is the result of exchange averaging of the ^{129}Xe environment in $XeOSO_2F^+$ with a high proportion of $Xe(OSO_2F)_2$; the exchange-averaged resonance consequently occurs at higher field than that of $XeOSO_2F^+$ in acidified media. The addition of AsF_5 to these solutions appears to almost completely shift equilibrium 20 to the left by the formation of high concentrations of the acidium ion, $H_2SO_3F^+$, according to equilibrium 21, where

$$nAsF_5 + 2HSO_3F \rightleftarrows H_2SO_3F^+ + [(AsF_5)_nSO_3F]^- \quad (21)$$

n = 1 or 2. In the absence of AsF_5, the low-field $XeOSO_2F^+/Xe(OSO_2F)_2$ peak collapses into the base line at −66 to −50 °C owing to slowing of the fast xenon exchange by further shifting of equilibrium 20 to the left, i.e., increasing the relative concentration of $XeOSO_2F^+$. As the relative concentration of $XeOSO_2F^+$ continues to increase at higher temperatures, rapid xenon exchange resumes, and the exchange-averaged line sharpens and again becomes visible, but at lower field than previously observed, reflecting the increased proportion of $XeOSO_2F^+$. As part of the normal temperature dependence, the chemical shift of this line continues to decrease with increasing temperature along with that of $XeOTeF_5^+$.

At higher temperatures and initial concentrations of $XeOTeF_5^+$, equilibrium 20 is effectively suppressed and equilibrium 16 dominates (Table IV). Consequently, the ^{129}Xe spectra of saturated solutions between −32 and +3 °C (Table IV) exhibit the same but less dramatic chemical shift reversal of the low-field peak, whose chemical shift now occurs at consistently lower fields than previously observed. This peak (ca. −1290 ppm) may consequently be assigned to $XeOSO_2F^+$ itself.

The decomposition of $XeOSO_2F^+$ has been monitored by ^{19}F and ^{129}Xe NMR spectroscopy. Successive warmings of the ^{19}F NMR samples to room temperature followed by quenching to −80 °C showed that decomposition occurred over a period of approximately $2^1/_2$ h to give $HOTeF_5$, $S_2O_6F_2$, XeF^+ cation,[26] and xenon gas. It is clear, however, that $HOTeF_5$ initially present in the unwarmed samples arises from equilibrium 16 and does not arise from the aforementioned decomposition, as no $S_2O_6F_2$ line is present in the spectra of the unwarmed solutions. The corresponding ^{129}Xe data are given in Table V and are consistent with the ^{19}F NMR findings and the decomposition reaction represented by eq 22. Ex-

$$2XeOSO_2F^+AsF_6^- \rightarrow Xe + XeF^+AsF_6^- + AsF_5 + S_2O_6F_2 \quad (22)$$

change averaging of the xenon environments XeF^+ and $XeOSO_2F^+$ according to eq 23 was found to occur and is

$$*XeOSO_2F^+ + XeF^+ \rightarrow XeOSO_2F^+ + *XeF^+ \quad (23)$$

consistent with a time-dependent shift to low field observed for the low-field peak as the relative proportion of XeF^+ increased throughout decomposition (cf. XeF^+ as the $Sb_2F_{11}^-$ compound in HSO_3F solvent at −70 °C; $\delta_{^{129}Xe}$ −911, $J_{^{129}Xe-^{19}F}$ = 6703 Hz).[25]

Apparatus and Materials. All manipulations were carried out under anhydrous conditions on a vacuum line constructed from 316 stainless steel, nickel, Teflon, and FEP. Bromine pentafluoride and arsenic pentafluoride were transferred under

Table V. ^{129}Xe NMR Study of the Decomposition of $XeOTeF_5^+AsF_6^-/XeOSO_2F^+AsF_6^-$ Equilibrium Mixtures in HSO_3F Solvent

time, min[a]	temp, °C	cation	$\delta_{^{129}Xe}$
0	−18	$XeOSO_2F^+$	−1296
		$XeOTeF_5^+$	−1592
	−51	$XeOTeF_5^+$	−1566
	−74		−1550
	−80		−1546
10	−18	$XeF^+/XeOSO_2F^+$	−1267[b]
		$XeOTeF_5^+$	−1587
28	−18	$XeF^+/XeOSO_2F^+$	−1076[b]
		$XeOTeF_5^+$	−1564
	−80	XeF^+	−924[c]
		$XeOTeF_5$	−1520
60	−18	XeF^+	−991[c]
		$XeOTeF_5^+$	−1536
	−80	XeF^+	−932[c]
		$XeOTeF_5^+$	−1529

[a] At 25 °C; initial concentration of $XeOTeF_5^+AsF_6^-$ 0.802 *m*. [b] ^{129}Xe environments are exchange averaged. [c] $J_{^{129}Xe-^{19}F}$ = 6350 Hz.

vacuum through Kel-F and Teflon connections previously passivated with fluorine. Antimony pentafluoride and fluorosulfuric acid were syringed into sample tubes in a drybox. All small-scale preparative work involving xenon compounds was carried out in 7 or 10 mm o.d. lengths of FEP spaghetti tubing heat sealed at one end and connected through 45° SAE flares to Kel-F valves.

Antimony pentafluoride (Ozark-Mahoning) was purified by double distillation in an atmosphere of dry nitrogen with use of an all-glass apparatus and stored in FEP vessels in a drybox.

Bromine pentafluoride (Matheson) was distilled into a Kel-F bubbler fitted with Teflon valves and purified by passing fluorine at atmospheric pressure through the liquid until all the Br_2 and BrF_3 had reacted. After degassing, BrF_5 was vacuum distilled and stored over dry NaF in a Kel-F storage vessel until used.

Fluorosulfuric acid (Baker and Adamson) was purified by the standard literature method.[29]

Arsenic pentafluoride was prepared by the direct interaction of arsenic powder (K and K Laboratories) with a 20% excess of fluorine (Matheson) initially at −196 °C followed by heating at 150 °C for 8 h. Prior to fluorinating the arsenic, As_2O_3 surface contaminant was sublimed from the commercial sample of arsenic by heating at 210 °C under vacuum for 2 days.

The preparations of XeF_2,[30] $HOTeF_5$,[31] $Xe(OTeF_5)_2$,[3] $FXeOTeF_5$,[4] and $XeOTeF_5^+AsF_6^-$[5] have been described elsewhere.

$XeOTeF_5^+Sb_2F_{11}^-$. The title compound was prepared by displacement of AsF_5 from the AsF_6^- compound. In a typical preparation, 0.798 g (1.428 mmol) of $XeOTeF_5^+AsF_6^-$ was dissolved in 3.23 g (14.9 mmol) of SbF_5, resulting in a yellow-orange solution at room temperature. Arsenic pentafluoride and excess SbF_5 were removed under vacuum at room temperature, yielding 1.161 g (theoretical 1.174 g) of a light yellow-orange solid corresponding to $XeOTeF_5^+Sb_2F_{11}^-$.

$XeF_2 \cdot BrOF_2^+AsF_6^-$. In a typical preparation, solid $XeF_2 \cdot BrOF_2^+AsF_6^-$ was prepared by dissolving 0.266 g (0.476 mmol) of $XeOTeF_5^+AsF_6^-$, contained in a 7 mm o.d. FEP reaction vessel, in 0.50 g (2.9 mmol) of BrF_5 at −48 °C. Warming to room temperature resulted in a rapid color change from a straw yellow to a colorless solution along with the evolution of TeF_6 gas. The reaction mixture was held at room temperature for approximately 1 min to ensure complete reaction and cooled to −48 °C, and TeF_6 and BrF_5 were removed under vacuum. The resulting white to very pale yellow solid was stored at −78 °C until its Raman spectrum could be recorded.

Sample Preparations. Nuclear magnetic resonance samples were prepared in 10 mm o.d. (^{17}O), 8 mm o.d. (^{129}Xe and ^{125}Te), or 5 mm o.d. (^{19}F) precision glass NMR tubes (Wilmad) joined to $^1/_4$ in. o.d. standard wall tubing and attached by means of $^1/_4$ in. Teflon nuts and ferrules to a Teflon diaphragm valve.[32] Samples containing BrF_5 solvent were prepared by distilling BrF_5 through all Kel-F and Teflon connections into a sample tube containing the solute at −196 °C. Fluorosulfuric acid and SbF_5 samples were prepared in a drybox by syringing the solvent into a sample tube containing the solute at −196 °C. Samples were warmed briefly at −48 °C to effect dissolution, with the exception of samples containing SbF_5 as a solvent; these were warmed to room temperature.

All Raman spectra were obtained in 5 mm o.d. precision glass NMR tubes with the exception of $XeF_2 \cdot BrOF_2^+AsF_6^-$. The Raman spectrum of the latter compound was recorded in the original 7 mm o.d. FEP reaction vessel.

All Raman and NMR samples were stored at −196 °C until their spectra could be recorded.

Nuclear Magnetic Resonance. Nuclear magnetic resonance spectra were obtained on natural-abundance compounds with use of a Bruker WH-90 Fourier-transform multinuclear spectrometer equipped with a Nicolet 1080 computer, a Nicolet 294 disk memory, and quadrature-phased detection. All spectra were ^2H-locked and accumulated in 16K of memory with the exception of ^{17}O spectra which were accummulated in 8K of memory. Fluorine-19 spectra were obtained at 84.66 MHz in 300–400 scans with a spectral width of 15 kHz (1.8 Hz/data point, pulse repetition time = 0.540 s) and a pulse width of 2 μs. Xenon-129 and tellurium-125 spectra were obtained at 24.90 and 28.43 MHz in 5000–50 000 scans and 100 000–200 000 scans, respectively, with spectral widths of 50 kHz (6.2 Hz/data point, pulse repetition time = 0.16 s) and pulse widths of 25 μs. The high-field ^{129}Xe NMR spectrum of $FXeFXeOTeF_5^+$ (Figure 5b) was obtained at 69.20 MHz with use of a Bruker WM-250 spectrometer (32K memory, 2000 scans, 100-kHz spectral width, 6.2 Hz/data point, 0.16-s repetition time, 25-μs pulse width). Line broadenings of 0.1 (^{19}F), 5 (^{129}Xe), and 10 Hz (^{125}Te) were applied in the exponential smoothing of the free induction decays. Fluorine-19 spectra were recorded in a 5 mm o.d. probe insert and locked to an external D_2O capillary in the probe-head housing. Xenon-129 (24.90 MHz) and tellurium-125 spectra were obtained in 8 mm o.d. NMR tubes placed inside 10 mm o.d. tubes and a 10-mm probe insert. The annular tube space was used to contain the external ^2H-lock substance which was D_2O at ambient temperature and acetone-d_6 at low temperatures. High-field ^{129}Xe spectra were run unlocked in 10 mm o.d. tubes. NMR spectra were fitted with use of a Nicolet 1080 computer system and the program ITRCAL.[34] In cases involving AB_4 and AB_4X spin systems, the origin of each spectrum was located, and the transitions (theoretically 25) were numerically assigned and approximate values of $J_{F_a-F_e}$ and $\nu_0\delta_{F_a-F_e}$ obtained as in ref 33. The crude

(29) Barr, J.; Gillespie, R. J.; Thompson, R. C. *Inorg. Chem.* **1964**, *3*, 1149.
(30) Williamson, S. M. *Inorg. Synth.* **1968**, *11*, 147.
(31) Seppelt, K.; Nöthe, D. *Inorg. Chem.* **1973**, *12*, 2727.
(32) Schrobilgen, G. J. Ph.D. Thesis, McMaster University, Hamilton, Ontario, Canada, 1974.
(33) The relationship $\Sigma(11,12) = \Sigma(13,14) = \Sigma(15,16) = \Sigma(19,20) = 2\nu_0\delta_{AB}$ was used to determine the approximate separation in Hz between environments A and B of the AB_4 spectra. The expression $\Sigma(i,j)$ represents the sum of the frequencies of the *i*th and *j*th transitions relative to the origin (the chemical shift of environment A, transition number 6). This relation is incorrectly stated in: Bladon, P.; Brown, D. H.; Crosbie, K. D.; Sharp, D. W. A. *Spectrochim. Acta, Part A* **1970**, *26A*, 2221.
(34) "Iteration of Calculated NMR Spectra Using Least Squares Criteria (ITRCAL)"; Nicolet Instrument Corp., Madison, Wis., 1974.

values of $J_{F_a-F_e}$ and the relative chemical shifts together with the experimental transitions were then iterated with use of ITRACL to give the best fit for the experimentally observed set of transitions. Root-mean-square errors of less than 1.0 Hz were achieved in one or two iterations.

Variable-temperature studies were carried out with use of a Bruker temperature controller. Temperatures were measured with a copper–constantan thermocouple inserted directly into the sample region of the probe and were accurate to ±1 °C.

Laser Raman Spectroscopy. A Spectra Physics Model 164 argon-ion laser giving up to 900 mW at 5145 Å was used to excite the Raman spectra. The spectrometer was a Spex Industries Model 14018 double monochromator equipped with 1800 groves/mm Holographic gratings. An RCA C31034 phototube detector in conjunction with a pulse count system consisting of pulse amplifier, analyzer, and ratemeter (Hamner NA-11, NC-11, and N-780A, respectively) and a Texas Instruments Model FSOZWBA strip chart recorder were used to record the spectra. The spectrometer was periodically calibrated by recording the discharge lines from an argon lamp over the spectral range of interest; the Raman shifts quoted are estimated to be accurate to ±1 cm^{-1}. Slit widths depended on the scattering efficiency of the sample, laser power, etc., with 1.3 cm^{-1} being typical.

Cylindrical sample tubes were mounted vertically. The angle between the incident laser beam and the sample tube was 45°, and Raman scattered radiation was observed at 45° to the laser beam or 90° to the sample tube direction.

Low-temperature spectra were recorded at −196 °C by mounting the sample vertically in an unsilvered Pyrex glass Dewar filled with liquid nitrogen.

Registry No. $XeOTeF_5^+AsF_6^-$, 27680-14-4; $XeOTeF_5^+Sb_2F_{11}^-$, 77079-64-2; $XeF_2 \cdot BrOF_2^+AsF_6^-$, 77071-47-7; $FXeFXeOTeF_5^+$, 77079-65-3; $XeOSO_2F^+$, 77070-48-5; $Xe(OTeF_5)_2$, 25005-56-5; SbF_5, 7783-70-2; BrF_5, 7789-30-2; $HOSO_2F$, 7789-21-1; $BrOF_2^+$, 62521-26-0; $BrOF_3$, 61519-37-7; $(FXe)_2F^+$, 37366-73-7; $HOTeF_5$, 57458-27-2; $Xe(OSO_2F)_2$, 25523-77-7; XeF^+, 47936-70-9; TeF_6, 7783-80-4; AsF_5, 7784-36-3.

Contribution from the Department of Chemistry, Northwestern University, Evanston, Illinois 60201

Uranium Hexamethoxide and Mixed Methoxyuranium(VI) Fluorides: Facile Syntheses from UF_6 and a Nuclear Magnetic Resonance Investigation of Structure and Chemical Dynamics

EDWARD A. CUELLAR and TOBIN J. MARKS*

Received October 3, 1980

Efficient, one-step scalable syntheses of uranium hexamethoxide, $U(OCH_3)_6$, starting from readily available UF_6 and $NaOCH_3$ or $CH_3Si(OCH_3)_3$ are described. In addition, the reaction of appropriate quantities of $(CH_3)_3SiOCH_3$ or $U(OCH_3)_6$ with UF_6 produces a series of mixed methoxyuranium(VI) fluorides, $U(OCH_3)_nF_{6-n}$, $n = 1-5$, the degree of substitution being determined by control of stoichiometry. Characterization of the complexes by both ^1H and ^{19}F NMR indicates that all the species possess a monomeric, six-coordinate geometry and undergo rapid, intermolecular ligand exchange. A surprisingly large solvent and temperature dependence of the ^{19}F chemical shifts is interpreted in terms of charge-transfer complex formation. The solution-phase electronic spectrum of $U(OCH_3)_6$ is interpreted in terms of both ligand- and solvent-to-metal charge transfer.

Introduction

High-valent uranium alkoxides[1] are of current interest as organic medium-compatible precursors for new uranium compounds[2] and as subjects for isotopically selective infrared photochemical studies.[3,4] In particular, our recent success in laser-induced uranium isotope separation[4] using uranium hexamethoxide, $U(OCH_3)_6$, prompted the development of efficient syntheses for uranium hexaalkoxides and the related mixed methoxyuranium(VI) fluorides, as well as a detailed exploration of their chemical and physicochemical properties. Although the hexaalkoxides have been known for some time,[5] the existing syntheses are tedious and inefficient, typically requiring five steps starting from UCl_4.[5a] Also, little has been reported concerning the spectroscopic properties of these materials. We report here simple, one-step syntheses of $U(OCH_3)_6$ starting from UF_6. Other hexaalkoxides are then readily accessible by transalkoxylation[1,5] (eq 1). We also

$$U(OCH_3)_6 + \text{excess ROH} \rightarrow U(OR)_6 + 6CH_3OH \quad (1)$$

report here the syntheses of the new methoxyfluorouranium(VI) series $U(OCH_3)_nF_{6-n}$, $n = 1-5$. The interesting properties we demonstrate for these species include rapid intermolecular ligand exchange and an unusually large solvent and temperature dependence of the ^{19}F chemical shifts. The electronic spectrum of $U(OCH_3)_6$ and optical absorption trends of the $U(OCH_3)_nF_{6-n}$ series are interpreted on the basis of the known

(1) (a) Bradley, D. C.; Mehrotra, R. C.; Gaur, D. P. "Metal Alkoxides"; Academic Press: New York, 1978. (b) Bradley, D. C. *Adv. Inorg. Chem. Radiochem.* **1972**, *15*, 259. (c) Bradley, D. C.; Fisher, K. J. *MTP Int. Rev. Sci.: Inorg. Chem., Ser. One* **1972**, *5*, 65.

(2) (a) Sigurdson, E. R.; Wilkinson, G. *J. Chem. Soc., Dalton Trans.* **1977**, 812. (b) Halstead, G. W.; Eller, P. G.; Asprey, L. B.; Salazar, K. *Inorg. Chem.* **1978**, *17*, 2967.

(3) (a) Coleman, J. H.; Marks, T. J. U.S. Patent 4 097 384, 1978; *Chem. Abstr.* **1978**, *89*, 170739c. (b) Marks, T. J.; Weitz, E.; Miller, S. S.; Ernst, R. D.; Day, V. W.; Secaur, C. A. "Abstracts of Papers", 173rd National Meeting of the American Chemical Society, New Orleans, LA, March 1977; American Chemical Society: Washington, DC, 1977; INOR 4.

(4) (a) Miller, S. S. Ph.D. Dissertation, Northwestern University, Evanston, IL, 1980. (b) Miller, S. S.; DeFord, D.; Marks, T. J.; Weitz, E. *J. Am. Chem. Soc.* **1979**, *101*, 1036. (c) Cuellar, E. A.; Miller, S. S.; Teitelbaum, R. C.; Marks, T. J.; Weitz, E., submitted for publication.

(5) (a) Jones, R. G.; Bindschadler, E.; Blume, D.; Karmas, G.; Martin, G. A., Jr.; Thirtle, J. R.; Yoeman, F. A.; Gilman, H. *J. Am. Chem. Soc.* **1956**, *78*, 6030. (b) Bradley, D. C.; Chatterjee, A. K. *J. Inorg. Nucl. Chem.* **1959**, *12*, 71.

0020-1669/81/1320-2129$01.25/0